

The effect of Bi_2O_3 compensation during thermal treatment on the crystalline and electrical characteristics of bismuth titanate thin films

Wei-Kuo Chia^a, Cheng-Fu Yang^b, Ying-Chung Chen^{a,*}

^a Department of Electrical Engineering, National Sun Yat-Sen University, Kaohsiung 804, Taiwan

^b Department of Chemical and Materials Engineering, National University of Kaohsiung, Kaohsiung 811, Taiwan

Received 20 April 2006; received in revised form 19 June 2006; accepted 26 October 2006

Available online 8 January 2007

Abstract

Bismuth titanate thin films are deposited on ITO/glass substrates by rf magnetron sputtering at room temperature using a $\text{Bi}_4\text{Ti}_3\text{O}_{12}$ ceramic target. The deposited $\text{Bi}_4\text{Ti}_3\text{O}_{12}$ films are annealed in a conventional furnace in ambient air for 10 min at temperatures ranging from 550 to 640 °C. One specimen is annealed in a crucible containing additional Bi_2O_3 compensation powder, while the other specimen is annealed in ambient air. XRD analysis shows that the crystal phases of films annealed with Bi_2O_3 powder are better than those of films annealed without Bi_2O_3 powder. Furthermore, the EDS results reveal that the bismuth weight percentage of the former is higher than that of the latter. SIMS analysis shows that the bismuth decreases near the surface of $\text{Bi}_4\text{Ti}_3\text{O}_{12}$ film annealed without Bi_2O_3 powder, but reveals a stable distribution throughout the film annealed with Bi_2O_3 powder. These results imply that bismuth is readily evaporated during the thermal treatment process, particularly from the region near the film surface. Finally, the dielectric and polarization properties of the thin films annealed with Bi_2O_3 powder are found to be superior to those of the films annealed in ambient air.

© 2006 Elsevier Ltd and Techna Group S.r.l. All rights reserved.

Keywords: $\text{Bi}_4\text{Ti}_3\text{O}_{12}$; Bi_2O_3 ; rf Sputtering; Dielectric constant; Polarization

1. Introduction

Ferroelectric bismuth titanate ($\text{Bi}_4\text{Ti}_3\text{O}_{12}$) thin film has a unique bismuth layer structure [1] and has attracted considerable interest on account of its excellent ferroelectric, electro-optical, and piezoelectric properties, which render it as an ideal candidate for applications such as nonvolatile random access memory (NVRAM), optoelectronic devices, and sensors [2–4]. Processing techniques such as chemical solution deposition (CSD) [5], rf sputtering [6], metallorganic chemical vapor deposition (MOCVD) [7], pulse laser deposition (PLD) [8], and molecular beam epitaxy (MBE) [9] have been used to make $\text{Bi}_4\text{Ti}_3\text{O}_{12}$ thin films. However, bismuth evaporates readily during the process of thermal treatment, which will lead to the degradation of crystal structure and electrical characteristics of the $\text{Bi}_4\text{Ti}_3\text{O}_{12}$ film. Therefore, bismuth excess is added in the source materials of $\text{Bi}_4\text{Ti}_3\text{O}_{12}$ film in order to compensate for the anticipated bismuth evaporation during thermal treatment [5,6,8].

However, using non-stoichiometric bismuth to compensate for bismuth evaporation is difficult since the amount of bismuth loss depends on the fabrication method and the fabrication parameters. $\text{Bi}_4\text{Ti}_3\text{O}_{12}$ thin films are generally fabricated using chemical solution deposition since the process consumes only limited quantities of raw material and the optimal level of excess bismuth can be determined by comparing the characteristics of various specimens fabricated with known additions of bismuth excess in the source materials. By contrast, in sputtering methods, fabricating the target is complex and the raw material powders are expensive. Therefore, it is impractical to manufacture a series of targets with non-stoichiometric bismuth to compare the characteristics of resulting thin films in order to assess the optimal bismuth addition.

Instead of adding excess bismuth in the source target, this study proposes a novel bismuth compensation method by using external Bi_2O_3 vapor. $\text{Bi}_4\text{Ti}_3\text{O}_{12}$ thin films are deposited on ITO/glass substrates at room temperature using an rf sputtering process with a stoichiometric $\text{Bi}_4\text{Ti}_3\text{O}_{12}$ ceramic source target. The resulting thin films are crystallized in a conventional furnace using a conventional thermal annealing (CTA) method. In the annealing process, some specimens were placed in a

* Corresponding author. Tel.: +886 7 5254121; fax: +886 7 6624284.

E-mail address: ycc@mail.ee.nsysu.edu.tw (Y.-C. Chen).

crucible containing an additional supply of Bi_2O_3 powder, while the other specimens were positioned outside the crucible. Annealing is performed for 10 min at temperatures ranging from 550 to 670 °C. The crystal characteristics, surface morphologies, compositional depth profiles, and the physical and electrical characteristics of the annealed thin films at various temperatures are compared and discussed.

2. Experimental

The substrates used in this study were HOYA NA-40 glass plates of thickness 0.7 mm, coated with indium-tin-oxide (ITO), which had sheet resistance of $15 \Omega/\square$ and thickness of 150 nm. Before the deposition process, the substrates were placed in an ultrasonic cleaner tank and cleaned in acetone, isopropyl alcohol and deionized water, respectively, to remove any particles or organisms adhered to their surfaces. $\text{Bi}_4\text{Ti}_3\text{O}_{12}$ thin films were then deposited on the ITO/glass substrates using an rf magnetron sputtering process performed at room temperature with a $\text{Bi}_4\text{Ti}_3\text{O}_{12}$ ceramic source target. The sputtering parameters are summarized in Table 1. Then the specimens were divided into two groups for crystallization, some specimens were placed inside a crucible with an additional supply of Bi_2O_3 powder (purity 99.5%), while the other specimens were positioned adjacent to the crucible within a conventional furnace, as shown Fig. 1. The experimental results evidenced that the ITO/glass substrate bent and the $\text{Bi}_4\text{Ti}_3\text{O}_{12}$ thin films were damaged as temperature reached to 670 °C. Accordingly, the thin film specimens were annealed for 10 min at temperatures ranging from 550 to 640 °C with a heating rate of 20 °C/min. The annealed thin films are approximately 300 nm in thickness. The crystal structures of thin films were examined using a SIEMENS D5000 X-ray

Table 1
Sputtering conditions for $\text{Bi}_4\text{Ti}_3\text{O}_{12}$ thin films on ITO/glass

Target	$\text{Bi}_4\text{Ti}_3\text{O}_{12}$, 2 in. diameter
Substrate	0.7 mm thickness, $15 \Omega/\square$ ITO glass
rf power density	3.95 W/cm^2
Atmosphere	Ar 99.99%
Working gas pressure	1 Pa
Substrate temperature	Room temperature
Deposition time	40 min

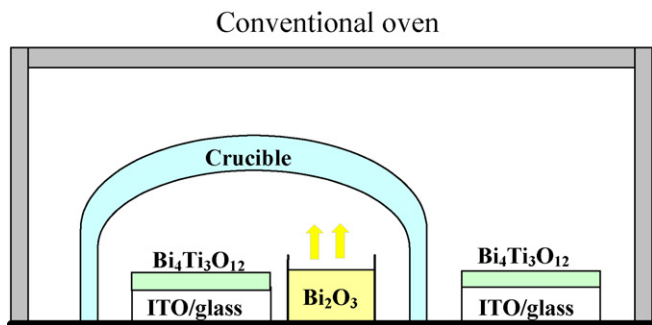


Fig. 1. Schematic diagram for the annealing of $\text{Bi}_4\text{Ti}_3\text{O}_{12}$ thin films in a conventional oven.

diffractometer (XRD) with Cu $K\alpha$ radiation and 2θ angle ranging from 20° to 60°. The surface morphologies were observed by field emission scanning electron microscopy (FE-SEM). Energy-dispersive spectroscopy (EDS) was used to examine the compositions of thin films. The depth profiles of the constituent elements of the films were characterized using a secondary ion mass spectrometer (SIMS). Aluminum was evaporated onto the surface of the thin films to form top electrodes with a diameter of 1 mm to facilitate measurement of the electrical properties. An HP4294 impedance analyzer was used to measure the capacitance–voltage (C – V) characteristics of the thin films at frequencies ranging from 1 to 100 kHz. The relative dielectric constant of each film, ϵ_r , was obtained from the relationship $C = \epsilon_r \epsilon_0 (A/d)$. Finally, the P – E hysteresis characteristics of the $\text{Bi}_4\text{Ti}_3\text{O}_{12}$ thin films were investigated at room temperature using an RT 66A ferroelectric tester with a triangle wave of $V_{pp} = 10 \text{ V}$ and a frequency of 50 kHz.

3. Results and discussion

Fig. 2(a) and (b) presents the XRD patterns of $\text{Bi}_4\text{Ti}_3\text{O}_{12}$ thin films annealed at various temperatures without and with additional Bi_2O_3 powder beside, respectively. At the temperature of 550 °C, the XRD patterns of the two specimens are similar, and the $\text{Bi}_4\text{Ti}_3\text{O}_{12}$ main phase peak (1 1 7) ($2\theta = 30.05^\circ$) and the ITO (2 2 2) ($2\theta = 30.18^\circ$) phase peak are superimposed. This result indicates that the temperature of 550 °C is not sufficient to crystallize the $\text{Bi}_4\text{Ti}_3\text{O}_{12}$ film, and no Bi_2O_3 vapor generated to compensate the evaporation loss of bismuth either. At 580 °C annealing temperature, there is no significant difference in the XRD patterns from that obtained at 550 °C for the films annealed without Bi_2O_3 . However, in Fig. 2(b), the $\text{Bi}_4\text{Ti}_3\text{O}_{12}$ (1 1 7) peak and the ITO (2 2 2) peak are separated slightly, which suggests that Bi_2O_3 vapor begins to compensate for the bismuth evaporation at this temperature. At the annealing temperature of 610 °C, the $\text{Bi}_4\text{Ti}_3\text{O}_{12}$ (1 1 7) peak in Fig. 2(b) is stronger and sharper, which indicates that this temperature is sufficiently high to form polycrystalline bismuth titanate. Meanwhile, the Bi_2O_3 vapor produced at this temperature fills the crucible and compensates for the evaporation loss of bismuth from the $\text{Bi}_4\text{Ti}_3\text{O}_{12}$ thin film, causing the Bi content to be closer the stoichiometric $\text{Bi}_4\text{Ti}_3\text{O}_{12}$ film. Although the (1 1 7) phase peak is also apparent above 610 °C in Fig. 2(a), it is not as sharp as that in Fig. 2(b). The results imply that the Bi_2O_3 vapor can enhance the crystallization of $\text{Bi}_4\text{Ti}_3\text{O}_{12}$ film when the temperature is higher than 580 °C.

Fig. 3(a) and (b) presents the SEM surface morphologies of $\text{Bi}_4\text{Ti}_3\text{O}_{12}$ thin films annealed without and with additional Bi_2O_3 powder, respectively, at the temperature of 610 °C. In Fig. 3(a), the surface morphology consists of circular grains of approximately 30–70 nm. However, Fig. 3(b) shows that the surface morphology of film has a compact, crack-free-structure consisting of oval and plate-shaped grains of size 100–150 nm. The results suggest that annealing with Bi_2O_3 at 610 °C can enhance the grain growth of thin films efficiently.

The variation of bismuth content in $\text{Bi}_4\text{Ti}_3\text{O}_{12}$ thin films is a function of annealing temperature, as shown in Fig. 4. For the

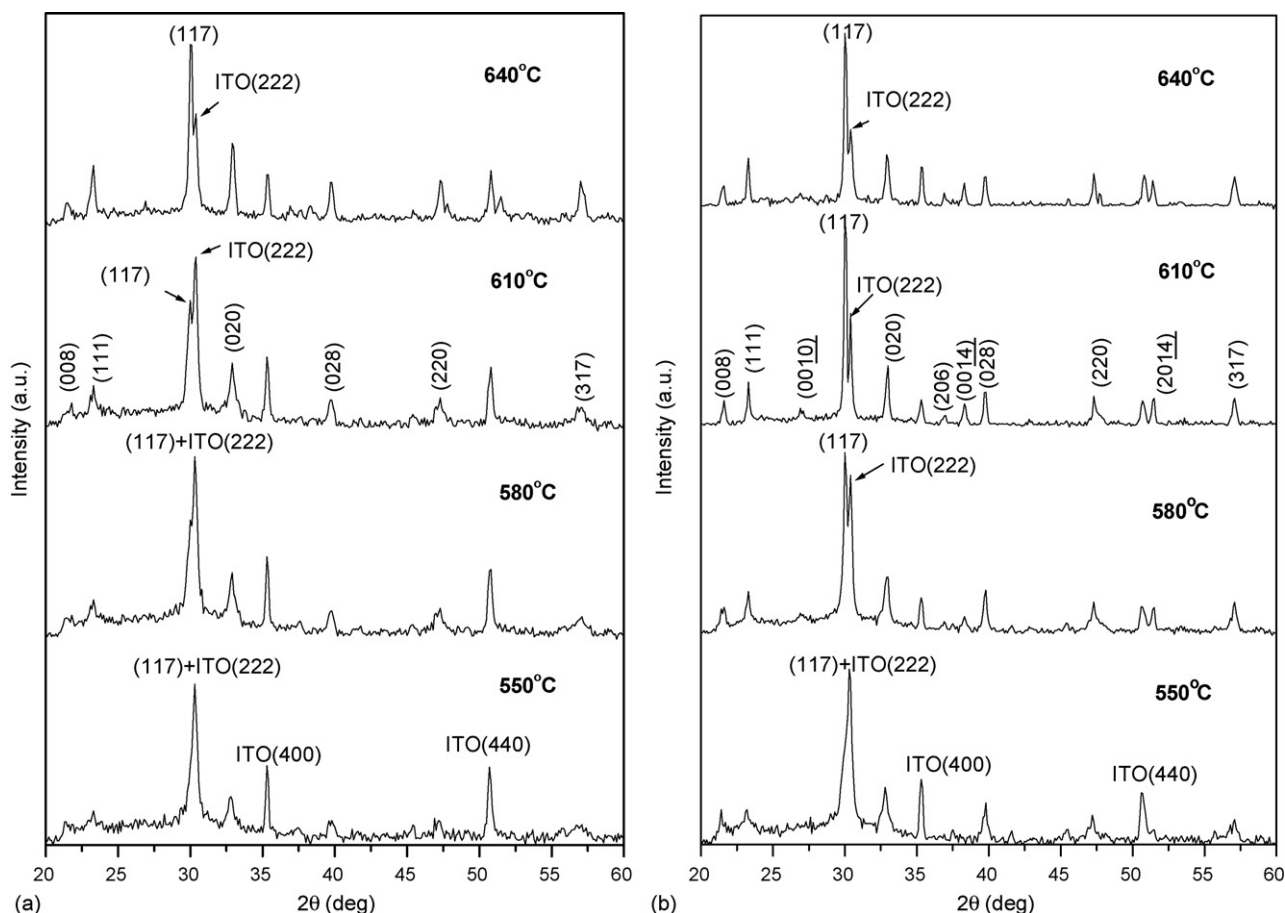


Fig. 2. XRD patterns of $\text{Bi}_4\text{Ti}_3\text{O}_{12}/\text{ITO}/\text{glass}$ annealed at various temperatures: (a) without additional Bi_2O_3 powder; (b) with additional Bi_2O_3 powder.

annealing temperature of 550 °C, the Bi weight percentage of the two specimens are similar, which is close to the value of 75.5 wt.% for both films, which suggests that the additional Bi_2O_3 powder has little influence at this temperature. However, the Bi content of the $\text{Bi}_4\text{Ti}_3\text{O}_{12}$ film annealed with Bi_2O_3 powder increases with the increase of annealing temperature. This reveals that the Bi_2O_3 vapor compensates for the evaporation loss of bismuth from $\text{Bi}_4\text{Ti}_3\text{O}_{12}$ thin films annealed at a temperature higher than 580 °C, and the compensation efficiency increases with increasing temperature. Conversely, the Bi content of $\text{Bi}_4\text{Ti}_3\text{O}_{12}$ film annealed without Bi_2O_3 powder decreases with the increase of temperature, which implies that bismuth evaporates from the $\text{Bi}_4\text{Ti}_3\text{O}_{12}$ thin film during thermal treatment, and the evaporated amount increases with the increase of temperature. The standard bismuth weight percentage of $\text{Bi}_4\text{Ti}_3\text{O}_{12}$ is 71.36%. However, the measured values of the specimens are all higher than 71.36%. This can be attributed that the EDS analysis is a quasi-quantitative analysis and fails to detect accurately the oxygen content of $\text{Bi}_4\text{Ti}_3\text{O}_{12}$.

The difference of the thicknesses of $\text{Bi}_4\text{Ti}_3\text{O}_{12}$ films under various annealing conditions is not distinct, all of them show a thickness of approximately 300 nm. Fig. 5 shows the SEM cross-sectional image of $\text{Bi}_4\text{Ti}_3\text{O}_{12}$ films annealed at 610 °C with additional Bi_2O_3 powder. The depth profiles of the

elements of $\text{Bi}_4\text{Ti}_3\text{O}_{12}$ films annealed at 610 °C without and with additional Bi_2O_3 powder are shown in Fig. 6(a) and (b). As shown in Fig. 6(a), the SIMS sputtering time of bismuth layer is approximately 250 s, and the deficient bismuth signal appears approximately at the beginning of the SIMS sputtering stage (75 s), it demonstrates that the bismuth content is deficient to a depth of approximately 90 nm from the film surface (as indicated in the dashed circle). However, it is apparent that bismuth does not evaporate from the inner regions of the film. The oxygen profile shows a similar trend as that of the bismuth, as shown in Fig. 6(a), which suggests that the bismuth may evaporate as the form of compound of bismuth and oxygen. Fig. 6(b) shows that the profiles of bismuth and oxygen near the surface of $\text{Bi}_4\text{Ti}_3\text{O}_{12}$ film are flatter than those in Fig. 6(a). This demonstrates that the Bi_2O_3 vapor at 610 °C successfully compensates for the loss of bismuth and oxygen near the surface of the $\text{Bi}_4\text{Ti}_3\text{O}_{12}$ thin film during thermal treatment.

Fig. 7(a) and (b) illustrates the variations of the dielectric constant and loss factor (loss $\tan \delta$) of $\text{Bi}_4\text{Ti}_3\text{O}_{12}$ films as a function of frequency. It is observed that the dielectric constants decrease and the loss factors (other than curve (d) in Fig. 7(b)) increase with increasing frequency. The C–V measurements show that the dielectric constant is strongly dependent on the annealing temperature. In general, at any given frequency, the

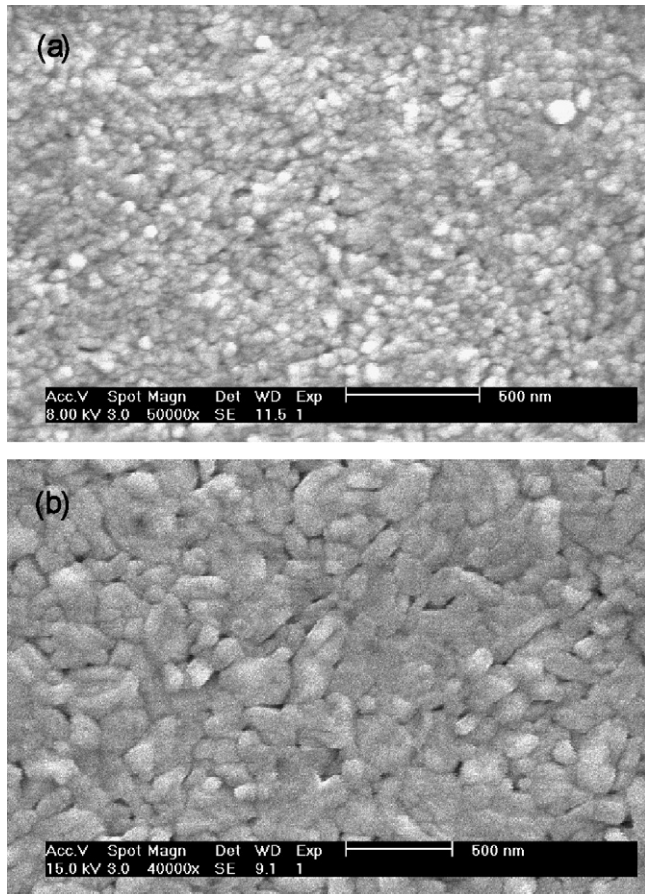


Fig. 3. SEM surface morphologies of $\text{Bi}_4\text{Ti}_3\text{O}_{12}$ /ITO/glass annealed at 610°C : (a) without additional Bi_2O_3 powder; (b) with additional Bi_2O_3 powder.

higher the annealing temperature is, the higher the dielectric constant and the greater the loss factor are. Comparing dielectric constant curves (a) in Fig. 7(a) and (b), in which the films are annealed at a temperature of 550°C , it can be observed that the dielectric constants of both films reduce from approximately 210 at 1 kHz to 190 at 100 kHz. However, at

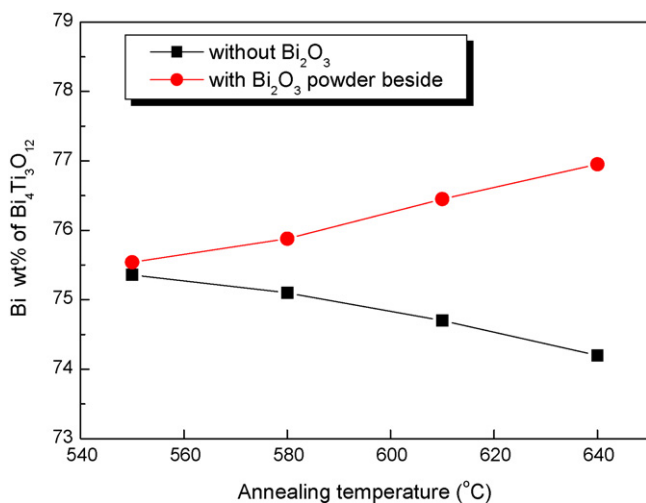


Fig. 4. Variation of bismuth wt.% of $\text{Bi}_4\text{Ti}_3\text{O}_{12}$ films annealed with and without additional Bi_2O_3 powder at temperatures of 550 – 640°C .

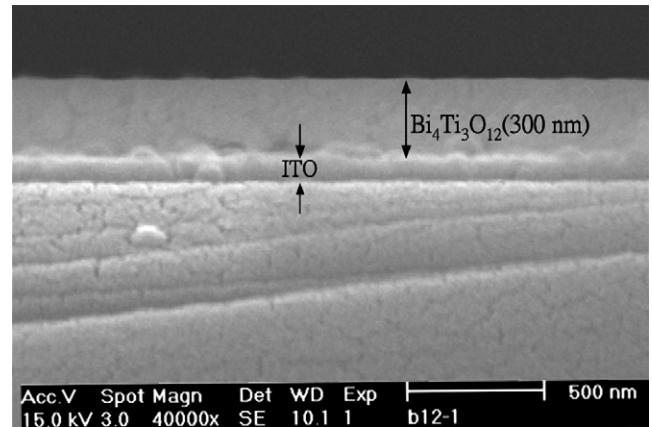


Fig. 5. Cross-section of $\text{Bi}_4\text{Ti}_3\text{O}_{12}$ /ITO/glass thin films annealed at temperature of 610°C with additional Bi_2O_3 powder.

annealing temperatures equal to or higher than 580°C , the dielectric constants of the films annealed with additional Bi_2O_3 powder are significantly higher than those of the films annealed without Bi_2O_3 , as shown in curves (b)–(d). The dielectric

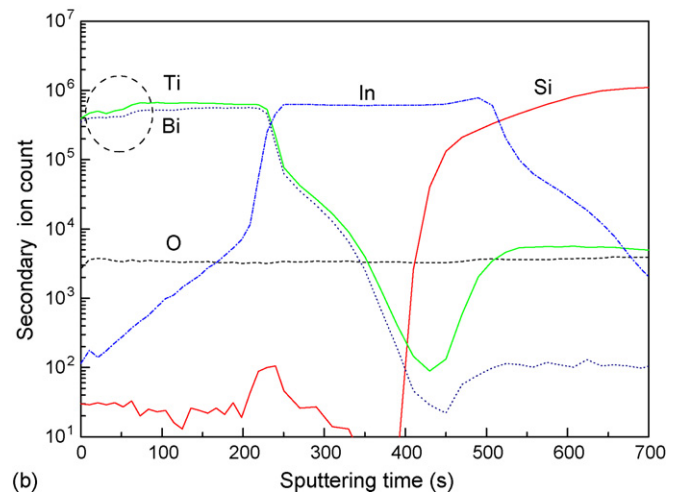
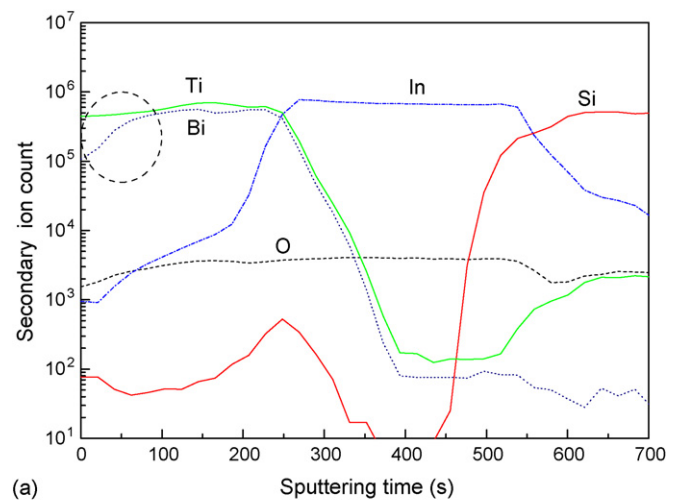


Fig. 6. SIMS depth profiles of $\text{Bi}_4\text{Ti}_3\text{O}_{12}$ /ITO/glass thin films annealed at temperature of 610°C : (a) without additional Bi_2O_3 powder; (b) with additional Bi_2O_3 powder.

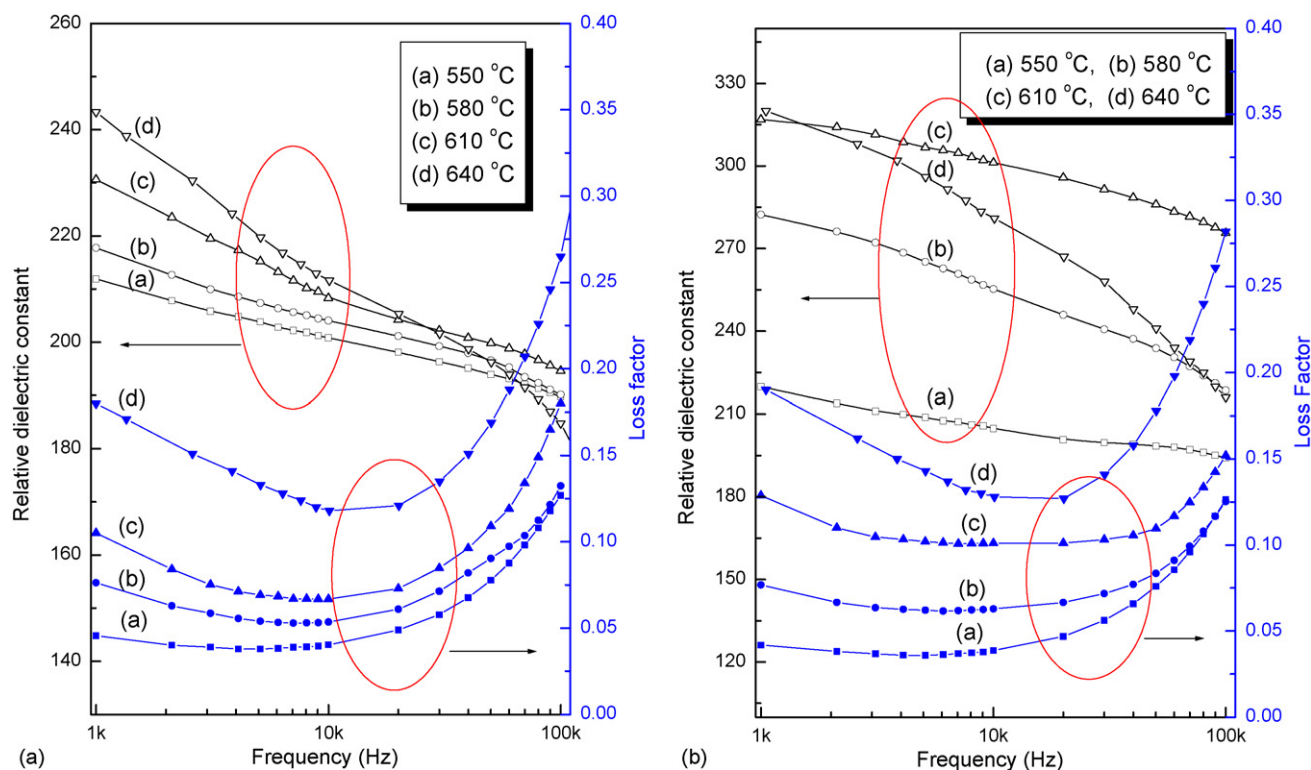


Fig. 7. Dielectric constants and loss factors of $\text{Bi}_4\text{Ti}_3\text{O}_{12}/\text{ITO}/\text{glass}$ annealed at various temperatures as a function of frequency: (a) without additional Bi_2O_3 powder; (b) with additional Bi_2O_3 powder.

constant of the film annealed with additional Bi_2O_3 powder at a frequency of 10 kHz is approximately 301 at 610 °C, whereas that of the film annealed in ambient is less than 212 at the same annealing temperature. These trends are consistent with the X-ray diffraction results presented in Fig. 2(a) and (b), i.e., a better crystallization phase of the film will contribute to the higher dielectric characteristics of the film. The poorer dielectric characteristics of the films annealed without additional Bi_2O_3 powder can be attributed to the lack of bismuth and the non-equilibrium structure of the film near the interface between the film and the substrate [10]. Interestingly, it is observed that the dielectric constants of the films in Fig. 7(a) and (b) decrease more rapidly with increasing frequency at temperature of 640 °C than at 610 °C. There are two likely reasons for this temperature-induced phenomenon: (1) enhanced interface diffusion between the $\text{Bi}_4\text{Ti}_3\text{O}_{12}$ layer and the ITO layer damages the conductance of the bottom electrode (ITO) and therefore influences the electrical characteristics, and (2) since the films are annealed in air rather than in a pure oxygen ambient, some impurities in the air and/or within the Bi_2O_3 powder are released and react with the thin films resulting in surface defects. Other than loss factor curve (d), the loss factor curves associated with the various annealing conditions are similar and the loss factors are less than 0.18. However, loss factor curves (d) reveal a distinct parabolic form, with a lowest value at 10 kHz in both specimens. The reason is not clear, but may be a result of film defects and/or electrode damage at high annealing temperatures.

Fig. 8 shows the P – E hysteresis loops of the $\text{Bi}_4\text{Ti}_3\text{O}_{12}$ thin films annealed at 610 °C. The film annealed without Bi_2O_3 powder exhibits an asymmetrical hysteresis loop with a remanent polarization (P_r) of 1.9 $\mu\text{C}/\text{cm}^2$ and a coercive field (E_c) of 79 kV/cm. However, a more symmetrical and saturated hysteresis loop with $P_r = 3.7 \mu\text{C}/\text{cm}^2$ and $E_c = 82 \text{ kV}/\text{cm}$ is obtained for the film annealed with Bi_2O_3 powder. Therefore, it is apparent that the supply of additional Bi_2O_3 during thermal treatment yields a distinct improvement in the ferroelectric properties of the film.

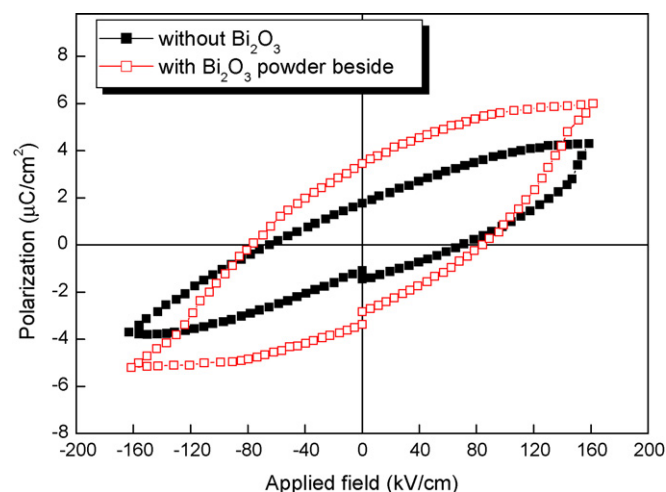


Fig. 8. P – E hysteresis loops of $\text{Bi}_4\text{Ti}_3\text{O}_{12}/\text{ITO}/\text{glass}$ annealed at 610 °C with and without additional Bi_2O_3 powder.

4. Conclusion

This study has identified a reduction in the bismuth content of $\text{Bi}_4\text{Ti}_3\text{O}_{12}$ thin films from the film surface during thermal treatment. The lack of bismuth in the $\text{Bi}_4\text{Ti}_3\text{O}_{12}$ film degrades its crystallinity, surface microstructure and electrical properties. However, the supply of additional Bi_2O_3 powder during the annealing process effectively compensates for the evaporation loss of bismuth of $\text{Bi}_4\text{Ti}_3\text{O}_{12}$ film above the temperatures of 580 °C. The $\text{Bi}_4\text{Ti}_3\text{O}_{12}$ thin films annealed with additional Bi_2O_3 beside possess superior crystal characteristics and surface morphologies compared to those of films annealed without Bi_2O_3 powder under the same annealing conditions. Furthermore, the difference between the bismuth content of the two specimens is found to increase with increasing annealing temperature. It demonstrates that the compensation efficiency of Bi_2O_3 increases with the increase of annealing temperature. The thin film annealed with additional Bi_2O_3 at 610 °C has the largest dielectric constant of 301 at the frequency of 10 kHz. By comparison, the dielectric constant of the film annealed without Bi_2O_3 under the same conditions is only 210. It is found that the dielectric constant of the film annealed with additional Bi_2O_3 is enhanced

by approximately 40–42% for frequencies in the range 1 k–100 kHz. Moreover, the remanent polarization of the film is also enhanced by approximately 65% compared to the film annealed without Bi_2O_3 , i.e., $P_r = 3.7 \mu\text{C}/\text{cm}^2$ compared to $P_r = 1.9 \mu\text{C}/\text{cm}^2$, respectively. Therefore, it can be concluded that the supply of additional Bi_2O_3 powder in the annealing process improves not only the crystalline characteristics of the $\text{Bi}_4\text{Ti}_3\text{O}_{12}$ thin film, but also its electrical properties.

References

- [1] T. Takenaka, K. Sakata, Jpn. J. Appl. Phys. 19 (1980) 31.
- [2] M. Yamaguchi, T. Nagatomo, O. Omoto, Jpn. J. Appl. Phys. 34 (1995) 5116.
- [3] X.S. Wang, J.W. Zhai, L.Y. Zhang, X. Yao, Infrared Phys. Technol. 40 (1999) 55.
- [4] D. Damjanovic, M. Demartin, H.S. Shulman, M. Testorf, N. Setter, Sensors Actuat. A53 (1996) 353.
- [5] L. Pintilie, I. Pintilie, M. Alexe, J. Eur. Ceram. Soc. 19 (1999) 1473.
- [6] M. Yamaguchi, T. Nagatomo, Thin Solid Films 348 (1999) 294.
- [7] T. Kijima, H. Matsunaga, Jpn. J. Appl. Phys. 38 (1999) 2281.
- [8] Y.N. Oh, S.G. Yoon, Appl. Surf. Sci. 227 (2004) 187.
- [9] S. Migita, H. Ota, H. Fujino, Y. Kasai, S. Sakai, J. Cryst. Growth 200 (1999) 161.
- [10] T.S. Kim, M.H. Oh, C.H. Kim, Thin Solid Films 254 (1995) 273.